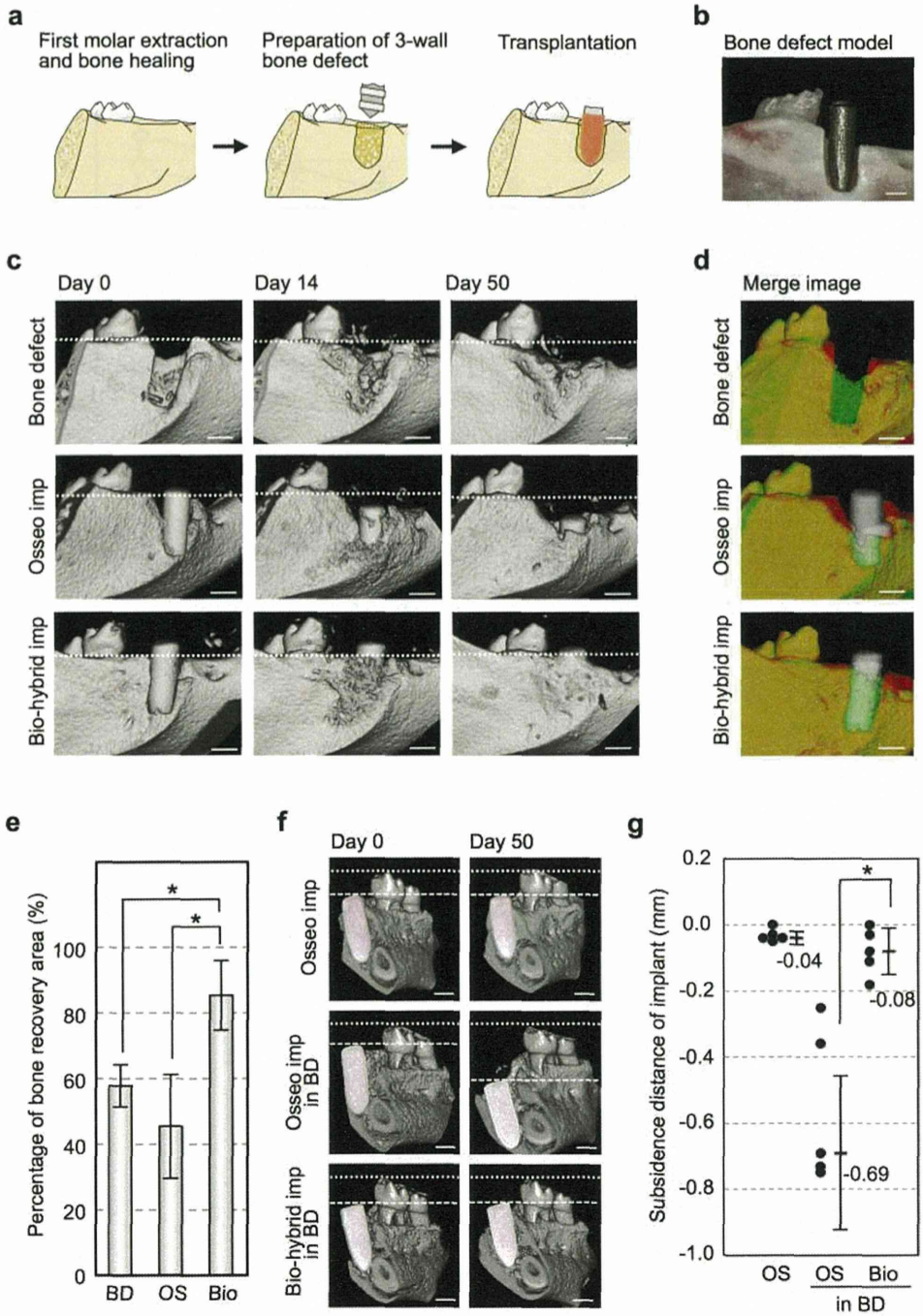

Figure 4 | Alveolar bone regeneration by transplantation of a bio-hybrid implant. (a) Schematic representation of the development of a murine 3-wall bone defect model and transplantation of the implant. (Drawings by C.T.) (b) Photographic representation of a murine 3-wall bone defect model and transplantation of the implant. Scale bar, 500 μm. (c) Micro-CT images of vertical alveolar bone regeneration processes in the bone defect without an implant (*top*), with transplantation of an osseo-integrated implant (*middle*) and with the transplantation of a bio-hybrid implant (*bottom*). Vertical bone formation was observed with the bio-hybrid implant, and the bone had recovered almost completely 50 days after transplantation. The superior edges of the recipient alveolar bone are indicated by a dotted line. Scale bar, 500 μm. (d) Three-dimensional superposition of micro-CT images for the non-treated control (*top*), the osseo-integrated implant (*middle*) and the bio-hybrid implant (*bottom*) in the 3-wall bone defect at 0 (red) and 50 days (green) after transplantation. Scale bar, 500 μm. (e) Regenerated bone area in the buccal region for the non-treated control (bone defect; BD), osseo-integrated implant (OS) and bio-hybrid implant (Bio) after 50 days in the 3-wall bone defect model. The data are presented as the mean ± s.d. with $n = 5$ for each experimental group. $^*p < 0.01$ (Bonferroni test). (f) Three-dimensional frontal micro-CT images of the subsidence of the osseo-integrated implant into normal tooth loss region (*upper*), osseo-integrated implant into the bone defect model (*middle*) and bio-hybrid implant into the bone defect model (*lower*). The height to the top of the second molar cusp is indicated by the dotted line, and the top of the implant is marked by a dashed line. Scale bar, 500 μm. (g) Vertical subsidence of the osseo-integrated implants in the normal tooth loss region (OS) and in the 3-wall bone defect model (OS in BD) as well as the bio-hybrid implants in the 3-wall bone defect model (Bio in BD) 50 days after transplantation. The data are presented as the median ± s.d. with $n = 5$ for each experimental group. $^*p < 0.01$ (Mann-Whitney U-test).

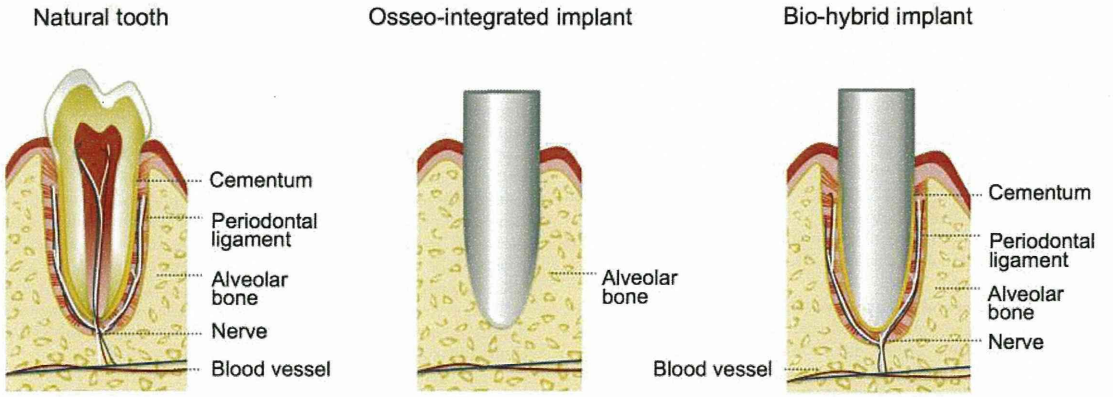

Figure 5 | Model of the connection to the periodontal tissues of a bio-hybrid implant. Schematic representation of the natural tooth, osseo-integrated implant and bio-hybrid implant. The bio-hybrid implant restored physiological functions, including bone remodelling, regeneration of severe bone-defect and responsiveness to noxious stimulations, through regeneration with periodontal tissues, such as cementum, PDL and alveolar bone. (Drawings by K.N.).

plantation, are difficult to apply to this clinical condition[37]. Although bone regenerative therapies have been attempted, including various utilisations of guided bone regeneration methods, autologous bone or cell transplantation and cytokine therapies[37,44], a clinical protocol for bone regeneration has not been available yet[36]. In this study, we demonstrated that a bio-hybrid implant induced vertical bone regeneration in a 3-wall bone defect model. These results suggest that the surrounding tissue, including alveolar bone, recognised the bio-hybrid implant as an equivalent organ to a natural tooth through its connection with the periodontal tissue on the surface of the titanium implant, which led to alveolar bone regeneration that was differentiated from the outer layer of dental follicle tissue after the transplantation. These findings indicate that transplantation of bio-hybrid artificial organs can achieve functional restoration and have the potential to restore the surrounding tissue via a mutual interaction between the bio-hybrid organ and the surrounding tissue.

Artificial organs with sensory functions, such as artificial eyes and cochlear implants, have been successfully used to restore visual and auditory functions via the proper afferent neurotransmission of external signals[5,6]. Furthermore, bio-hybrid artificial arms substituting arm locomotorium loss can reproduce arbitrary motions through efferent neurotransmission to an artificial machine[7]. Although these artificial therapies are effective and partially restore organ function, further technological improvements are required to exert biological organ functions via proper nerve innervations under the control of the CNS[5–7]. Teeth are peripheral target organs for the sensory trigeminal and sympathetic nerves, both of which play essential roles in tooth function and protection against noxious stimulations[12,34]. Current dental implant therapies are unable to receive the noxious stimulations due to a lack of interaction with the peripheral nerves and the periodontal tissue[15,16]. To recover the neuronal perception to mechanical forces, a next-generation bio-hybrid implant therapy that can fully restore the periodontal tissues is needed in the near future[11]. In the current study, we demonstrated that the successful innervation into the regenerated periodontal tissues around the bio-hybrid implant could restore responsiveness to noxious stimuli. These findings indicate that the transplantation of bio-hybrid artificial organ has great potential for the recovery of neuronal function via proper nerve innervations.

To realise future clinical applications of bio-hybrid implants, a suitable cell source must be identified. Current regenerative therapies for dental disorders have used stem cells derived from wisdom teeth/tooth germ tissue, such as the dental pulp, periodontal ligament, apical papillae and dental follicle, which have been shown to repair damaged tissues[45–48]. Currently, stem cells derived from the wisdom tooth (impacted third molar) germ of young patients, which can correspond to the ED18.5 dental follicle stem cells used here, are thought to be a potential candidate for periodontal tissue regeneration on a bio-hybrid implant[49,50]. The identification and the engineering optimisation of adult tissue stem cells useful for periodontal tissue regeneration will help develop a clinically relevant next-generation bio-hybrid implant therapy for treating tooth loss.

In conclusion, our study demonstrated a novel bio-hybrid implant with connected fibrous tissue as a bio-hybrid organ. This study represents a significant advancement in the development of a next-generation therapeutic for the treatment of tooth loss, as this bio-hybrid implant restored periodontal tissue structure and function through its fibrous tissue-based connection to the surrounding tissue.

Methods

Ethics statement of animal research. C57BL/6 and C57BL/6-TgN (act-EGFP) mice were purchased from SLC Inc., (Shizuoka, Japan). All handling and care of the mice conformed to the National Institute of Health (NIH) guidelines for animal research, and all experimental protocols involving animals were approved by the Tokyo University of Science Animal Care and Use Committee (Permit Number: N13010). All surgeries were performed under sodium pentobarbital anaesthesia, and all efforts were made to minimise suffering.

Tissue isolation and analysis of periodontal tissue formation. We extirpated the tooth germs at embryonic day (ED) 14.5, 18.5 and at postnatal day (PD) 7, and mature teeth were extracted at PD35. The isolated tooth germs were incubated in 50 U/ml dispase (BD, Franklin Lakes, NJ, USA) for 2 min at room temperature as a brief enzymatic treatment for the separation of the dental mesenchyme, or dental follicle tissue, from the tooth germ. After enzymatic treatment, the mesenchymal tissue and dental follicle tissues (DF) were separated using a fine needle in Dulbecco's modified Eagle's medium (D-MEM; Kohjin bio, Saitama, Japan) supplemented with 10% foetal calf serum (GIBCO, Grand Island, NY, USA), 100 U/mL penicillin (Sigma, St. Louis, MO, USA), 100 mg/mL streptomycin (Sigma) and 70 U/mL Deoxyribonuclease I from bovine pancreas (DNase I; Sigma). The periodontal ligament tissues were seceded from PD35 in the first molar using a surgical knife. Each of the isolated tissues were wrapped around hydroxyapatite particles (HA, CALCITITE; Hakuho, Tokyo, Japan) of approximately 50 μm in diameter. These HA particles were placed onto a cell culture insert (0.4 mm pore diameter; BD) and incubated at 37°C for 24 hours, and they were transplanted into a subrenal capsule for 30 days using syngeneic C57BL/6 mice (8 week-old, female) as the host.

***In situ* hybridization analysis.** *In situ* hybridisations were performed using 10 μm thick frozen sections. Digoxygenin-labelled probes for the specific transcripts were prepared by PCR using primers designed from published sequences (*F-spondin*, GenBank ID: NM_145584; *Periostin*, GenBank ID: NM_015784; *Osteocalcin* (*OCN*), GenBank ID: NM_007541; *Collagen type I* (*Col1*), GenBank ID: NM_007742; *Collagen type XVI alpha 1* (*Col16A*), GenBank ID: NM_028266; *Leprecan*, GenBank ID: NM_007541; *Nidogen-1* (*NID*), GenBank ID: NM_010917; *Scleraxis* (*Scx*), GenBank ID: NM_198885; *Tenascin-N* (*TNN*), GenBank ID: NM_177839; and *Colony-stimulating factor 1* (*Csf-1*), GenBank ID: NM_007778). The specific primers for these mouse genes were as follows: *F-spondin* (sense, 5′-AGACGGTCTACT-GGGCACTG-3′; antisense, 5′-TGCAAAAGGATGTGGT GGTA-3′), *Periostin* (sense, 5′-GGCTGAAGATGGTTCCTCTC-3′; antisense, 5′-CC ATGTGGCT-GTGTAAGGCATTC-3′), *OCN* (sense, 5′-AAGCCCAGCGACTCTGAGT CT-3′;

antisense, 5′-CCGGAGTCTATTCACCACCTTACT-3′), *Col1* (sense, 5′-CACT GCAAGAACAGCGTAGC-3′; antisense, 5′-TTGGTTTTTGGTCACGTTCA-3′), *Col16A* (sense, 5′-TACCTCCAGGATGCAGTTCC-3′; antisense, 5′-TCCTGTA-AGCTTTGG CCATT-3′), *Leprecan* (sense, 5′-GTCACAGGCTGAGAGGAAGG-3′; antisense, 5′-GC CCAGAGAAGAGTGTGTCC-3′), *NID* (sense, 5′-ACGTCA-TGGGAATCTTCAGC-3′; antisense, 5′-TGCAAACCGAACTTCTGATG-3′), *Scx* (sense, 5′-AAGAGGTGATGCC ACTAGTG-3′; antisense, 5′-TATACAAAAT-TTCCAGACTTTATATTATCAT-3′), *TNN* (sense, 5′-CAAGACCTGGAACA-GGGTGT-3′; antisense, 5′-TGCCTCTGTATTTCCCA ACC-3′), and *Csf-1* (sense, 5′-TACTGAACCTGCCTGCTGAA-3′; antisense, 5′-CC AGAGCTTGTGA-CAGGACA-3′). We superimposed images for *F-spondin*, *Periostin* and *OCN* staining using Adobe Photoshop software (Adobe Systems, San Jose, CA, USA).

Bio-hybrid implant fabrication and surface analysis. The implants were made of pure titanium wire (Nilaco, Tokyo, Japan) with a length of 1.7 mm and a diameter of 0.6 mm, and their apical sides were shaved into a conical shape. To promote cementum deposition around the implants, their surfaces were coated with HA, which is biocompatible and osteoinductive, via sputter deposition[32] (1–2 μm thickness of HA; Yamahachi dental MFG., Co., Aichi, Japan). DF tissues from ED18.5 mice were wrapped around the HA implants (5–6 tissues of each). The titanium and HA implants were coated with platinum, and their surfaces were observed using a S-4700 (Hitachi High-Tech, Tokyo, Japan) scanning electron microscope operated at 5 kV.

Transplantation of a bio-hybrid implant. The lower first molars of 4-week-old C57BL/6 mice were extracted under deep anaesthesia, and the resulting bone wounds were allowed to heal for 2–3 weeks. An incision of approximately 2.0 mm in length was made through the oral mucosa at the extraction site with a surgical knife to access the alveolar bone. A dental drill (NSK, Tochigi, Japan) and root canal files (MANI, Tochigi, Japan) were used to create a bony hole of approximately 0.8 mm in diameter and 1.3–1.5 mm in depth in the exposed alveolar bone surface. The HA and bio-hybrid implants were transplanted into the bony hole, and the incised oral mucosa was sutured with 8-0 nylon (Bear Medic, Chiba, Japan). To generate a critical size bone defect model (3-wall bone defect model) which could not heal spontaneously, the buccal supporting alveolar bone (0.7 mm in mesiodistal width and 1.5 mm in depth) in the lower first molar extracted region was removed using a dental drill under deep anaesthesia. The implants were transplanted into these defects using the same procedure described above.

Microcomputed tomography (Micro-CT). Radiographic imaging was performed by x-ray using a Micro-CT device (R_mCT; Rigaku, Tokyo, Japan) with exposure at 90 kV and 150 mA. Micro-CT images were captured using i-view R (Morita, Kyoto, Japan) and Imaris (Carl Zeiss, Oberkochen, Germany).

Histochemical analysis and immunohistochemistry. The tissues were excised and immersed in 10% formalin (Mildform 10 N; Wako, Osaka, Japan). After fixation, the tissues were decalcified in 10% sodium citrate and 22.5% formic acid for 3 days at 4°C. Tissue sections (5–8 μm) were made after embedding paraffin and were stained with either haematoxylin-eosin or azan. To visualise the elastic fibres, the sections were stained with a Resorcin-fuchsin solution (Muto Pure Chemicals, Tokyo, Japan) after 10% Oxone (Wako) treatment and then counterstained with 1% Orange G (Wako). The stained sections were observed using an Axioimager A1 microscope (Carl Zeiss) with an AxioCAM MRc5 (Carl Zeiss) camera. For fluorescent immunohistochemistry, 40 μm thick frozen sections were prepared and immunostained as previously described[35]. The sections were incubated with a primary antibody against the neurofilament SMI312 (1 : 1,000, mouse, Abcam, Cambridge, MA, USA). The primary antibody was detected using a highly cross-adsorbed Alexa Fluor® 594 Goat Anti-Rabbit IgG (H + L) (1 : 500, Life Technologies, Carlsbad, CA, USA). Fluorescence microscopy images were captured using a laser confocal microscope (LSM780; Carl Zeiss). To analyse the ability to perceive noxious stimulation by experimental orthodontic movement, we performed c-Fos immunohistochemistry as a pain response, which can be detected in the superficial layers of the medullary dorsal horn located in the brainstem[33,35]. The sections of the medullary dorsal horn in the brainstem region were incubated with anti-c-Fos Ab (1 : 10,000, Santa Cruz Biotechnology, Dallas, TX, USA). These sections were then immunostained with peroxidase-labelled goat anti-rabbit IgG (1 : 300, Cappel Laboratories, Cochranville PA, USA) and PAP immune complex (1 : 3,000, Cappel). The stained sections were observed on an Axiovert microscope (Carl Zeiss) equipped with an AxioCAM MRc5 camera (Carl Zeiss).

Electron microscopy and electron probe microanalysis. Each sample was fixed with 2.5% glutaraldehyde in 0.1 M phosphate buffer (pH 7.4) for 3 hours at 4°C. For SEM observations, samples were cut using a diamond disk and dehydrated in 100% ethanol. After coating with platinum, the samples were examined with a S-4700 SEM (Hitachi High-Tech) at 5 kV. For TEM analysis, the samples were post-fixed and embedded as a previously described[51]. Ultrathin sections were mounted on 150 mesh grids, stained with uranyl acetate and lead citrate and then examined by a H-7600 (Hitachi High-Tech) transmission electron microscope using an accelerating voltage of 75 kV. An electron probe microanalyzer (EPMA-1610; Shimadzu, Kyoto, Japan) was used for the elemental mapping of calcium (Ca), phosphorus (P), titanium (Ti), chlorine (Cl), magnesium (Mg), sodium (Na) and potassium (K). For the elemental analysis, undecalcified samples were embedded in epoxy resin and trimmed with diamond disks until the sagittal plane containing the centre of the implant was exposed. After polishing, the specimens were sputter-coated with carbon prior to elemental analysis.

Experimental orthodontic treatments. The orthodontic treatment was performed as described previously[33,35]. Experimental tooth movement was achieved with a horizontal orthodontic force of approximately 10–15 g that was applied continuously to the bio-hybrid implants of mice in the experimental group in the buccal direction using a dial tension gauge (Mitsutoyo, Kanagawa, Japan) for 3, 7 or 14 days. In the control group, the orthodontic force was applied in the buccal direction to the first molars of 7-week-old normal C57BL/6 mice in the same manner as the experimental group. Serial sections from day 6 samples were analysed by *in situ* hybridisation analysis for macrophage colony-stimulating factor-1 (*Csf-1*) and osteocalcin (*Ocn*) mRNA, as previously described[33,35]. The orthodontic movement distance of the bio-hybrid implants and natural first molars was measured using TRI/3D-BON software (Ratoc, Osaka, Japan).

Measurements of the regenerated bone area and subsidence distance of the implant. To evaluate the extent of alveolar bone regeneration in our buccal bone defect mouse model, we used a micro-CT device (Rigaku) to measure the alveolar bone area of the treated regions at 0 and 50 days post implantation. The area of the alveolar bone in the operated region was measured using Image J software (NIH, Bethesda, MD, USA). The alveolar bone area at day 50 was divided by the area at day 0 to calculate the regenerated bone area ratio. To analyse the subsidence of the implants in our buccal bone defect model, we measured the subsidence distance between the top of the second molar cusp and the top of the implant at 50 days post implantation. The vertical subsidence of implants is presented as the median ± standard deviation (s.d.).

Statistical analysis. Statistical significance was determined with a Bonferroni test and a Mann-Whitney *U*-test, and the data were analysed using the Common Gateway Interface Program (twk, Saint John's University).

1. Bengel, F. M. *et al.* Effect of sympathetic reinnervation on cardiac performance after heart transplantation. *N Engl J Med.* **345**, 731–738 (2001).
2. Copeland, J. G. *et al.* Cardiac Replacement with a Total Artificial Heart as a Bridge to Transplantation. *N Engl J Med.* **351**, 859–867 (2004).
3. Strain, A. J. & Neuberger, J. M. A bioartificial liver-state of the art. *Science* **295**, 1005–1009 (2002).
4. Davenport, A. *et al.* A wearable haemodialysis device for patients with end-stage renal failure: a pilot study. *Lancet* **370**, 2005–2010 (2005).
5. Kelly, S. K. *et al.* A hermetic wireless subretinal neurostimulator for vision prostheses. *IEEE Trans Biomed Eng.* **58**, 3195–3205 (2011).
6. Rauschecker, J. P. & Shannon, R. V. Sending Sound to the Brain. *Science* **295**, 1025–1029 (2002).
7. Kuiken, T. A. *et al.* Targeted reinnervation for enhanced prosthetic arm function. *Lancet* **369**, 371–380 (2007).
8. Huch, K. *et al.* Sports activities 5 years after total knee or hip arthroplasty: the Ulm Osteoarthritis Study. *Ann Rheum Dis.* **64**, 1715–1720 (2005).
9. Tomasek, J. J., Gabbiani, G., Hinz, B., Chaponnier, C. & Brown, R. A. Myofibroblasts and mechano-regulation of connective tissue remodeling. *Nat Rev Mol Cell Biol.* **3**, 349–363 (2002).
10. Avery, J. K. *Oral development and histology*. Steele, P. F. (ed.) 225–242 (Thieme Press, New York, 2002).
11. Shimono, M. *et al.* Regulatory mechanisms of periodontal regeneration. *Microsc Res Tech.* **60**, 491–502 (2003).
12. Proffit, W. R., Fields, H. W. & Sarver, D. M. *Contemporary orthodontics, 4th edition*. John, D. (ed.) 77–83 (Mosby Elsevier, St. Louis, 2006).
13. Rosenstiel, S. F., Land, M. F. & Fujimoto, J. *Contemporary fixed prosthodontics, 3rd edition*. John, S. & Penny, R. (ed.) 59–82 (Mosby, St. Louis, 2001).
14. Pokorny, P. H., Wiens, J. P. & Litvak, H. Occlusion for fixed prosthodontics: a historical perspective of the gnathological influence. *J Prosthet Dent.* **99**, 299–313 (2008).
15. Brenemark, P. I. & Zarb, G. A. *Tissue-integrated prostheses: osseointegration in clinical dentistry*. Albrektsson, T. (ed.) 211–232 (Quintessence Publishing Co, Inc, Chicago, 1985).
16. Burns, D. R., Beck, D. A. & Nelson, S. K. A review of selected dental literature on contemporary provisional fixed prosthodontic treatment: report of the Committee on Research in Fixed Prosthodontics of the Academy of Fixed Prosthodontics. *J Prosthet Dent.* **90**, 474–497 (2003).
17. Gault, P. *et al.* Tissue-engineered ligament: implant constructs for tooth replacement. *J Clin Periodontol.* **37**, 750–758 (2010).
18. Lin, Y. *et al.* Bioengineered periodontal tissue formed on titanium dental implants. *J Dent Res.* **90**, 251–256 (2011).
19. Ikeda, E. & Tsuji, T. Growing bioengineered teeth from single cells: potential for dental regenerative medicine. *Expert Opin Biol Ther.* **8**, 735–744 (2008).
20. Brockes, J. P. & Kumar, A. Appendage regeneration in adult vertebrates and implications for regenerative medicine. *Science* **310**, 1919–1923 (2005).
21. Segers, V. F. M. & Lee, R. T. Stem-cell therapy for cardiac disease. *Nature* **451**, 937–942 (2008).

22. Copelan, E. A. Hematopoietic stem-cell transplantation. *N Engl J Med.* **354**, 1813–1826 (2006).
23. Kim, J. H. *et al.* Dopamine neurons derived from embryonic stem cells function in an animal model of Parkinson's disease. *Nature* **418**, 50–56 (2002).
24. Elloumi-Hannachi, I., Yamato, M. & Okano, T. Cell sheet engineering: a unique nanotechnology for scaffold-free tissue reconstruction with clinical applications in regenerative medicine. *J Intern Med.* **267**, 54–70 (2010).
25. Sekine, H. *et al.* In vitro fabrication of functional three-dimensional tissues with perfusable blood vessels. *Nat Commun.* **4**, 1399 (2013).
26. Sasai, Y. Next-generation regenerative medicine: organogenesis from stem cells in 3D culture. *Cell stem cell* **12**, 520–530 (2013).
27. Silva, A. I., de Matos, A. N., Brons, I. G. & Mateus, M. An overview on the development of a bio-artificial pancreas as a treatment of insulin-dependent diabetes mellitus. *Med Res Rev.* **26**, 181–222 (2006).
28. Chen, W. *et al.* Restoration of auditory evoked responses by human ES-cell-derived otic progenitors. *Nature* **490**, 278–282 (2012).
29. Kitagawa, M., Ao, M., Miyauchi, M., Abiko, Y. & Takata, T. F-spondin regulates the differentiation of human cementoblast-like (HCEM) cells via BMP7 expression. *Biochem Biophys Res Commun.* **418**, 229–233 (2012).
30. Nishida, E. *et al.* Transcriptome database KK-Periome for periodontal ligament development: expression profiles of the extracellular matrix genes. *Gene* **404**, 70–79 (2007).
31. Thorfve, A. *et al.* Hydroxyapatite coating affects the Wnt signaling pathway during peri-implant healing *in vivo*. *Acta Biomater.* **10**, 1451–1462 (2014).
32. Ozeki, K., Yuhta, T., Fukui, Y., Aoki, H. & Nishimura, I. A functionally graded titanium/hydroxyapatite film obtained by sputtering. *J Mater Sci Mater Med.* **13**, 253–258 (2002).
33. Oshima, M. *et al.* Functional tooth regeneration using a bioengineered tooth unit as a mature organ replacement regenerative therapy. *PLoS One* **6**, e21531 (2011).
34. Dawson, P. E. *Functional occlusion: from TMJ to smile design.* John, D. (ed.) 18–26 (Mosby Elsevier, St. Louis, 2006).
35. Ikeda, E. *et al.* Fully functional bioengineered tooth replacement as an organ replacement therapy. *Proc Natl Acad Sci U S A.* **106**, 13475–13480 (2009).
36. Wise, G. E. & King, G. J. Mechanisms of Tooth Eruption and Orthodontic Tooth Movement. *J Dent Res.* **87**, 414–434 (2008).
37. Clementini, M., Morlupi, A., Canullo, L., Agrestini, C. & Barlattani, A. Success rate of dental implants inserted in horizontal and vertical guided bone regenerated areas: a systematic review. *Int J Oral Maxillofac Surg.* **41**, 847–852 (2012).
38. Araújo, M. G. & Lindhe, J. Dimensional ridge alterations following tooth extraction. An experimental study in the dog. *J Clin Periodontol.* **32**, 212–218 (2005).
39. Van der Weijden, F., Dell'Acqua, F. & Slot, D. E. Alveolar bone dimensional changes of post-extraction sockets in humans: a systematic review. *J Clin Periodontol.* **36**, 1048–1058 (2009).
40. Naert, I., Duyck, J. & Vandamme, K. Occlusal overload and bone/implant loss. *Clin Oral Implants Res.* **23**, 95–107 (2012).
41. Willer, J., Noack, N. & Hoffmann, J. Survival rate of IMZ implants: a prospective 10-year analysis. *J Oral Maxillofac Surg.* **61**, 691–695 (2003).
42. Kokubun, K., Kashiwagi, K., Yoshinari, M., Inoue, T. & Shiba, K. Motif-programmed artificial extracellular matrix. *Biomacromolecules* **9**, 3098–3105 (2008).
43. Yoshinari, M., Kato, T., Matsuzaka, K., Hayakawa, T. & Shiba, K. Prevention of biofilm formation on titanium surfaces modified with conjugated molecules comprised of antimicrobial and titanium-binding peptides. *Bio fouling.* **26**, 103–110 (2010).
44. Bueno, E. M. & Glowacki, J. Cell-free and cell-based approaches for bone regeneration. *Nat Rev Rheumatol.* **5**, 685–697 (2009).
45. Gronthos, S., Mankani, M., Brahim, J., Robey, P. G. & Shi, S. Postnatal human dental pulp stem cells (DPSCs) in vitro and in vivo. *Proc. Natl. Acad. Sci. U. S. A.* **97**, 13625–13630 (2000).
46. Seo, B. M. *et al.* Investigation of multipotent postnatal stem cells from human periodontal ligament. *Lancet* **364**, 149–155 (2004).
47. Sonoyama, W. *et al.* Characterization of the apical papilla and its residing stem cells from human immature permanent teeth: a pilot study. *J. Endod.* **34**, 166–171 (2008).
48. Huang, G. T., Gronthos, S. & Shi, S. Mesenchymal stem cells derived from dental tissues vs. those from other sources: their biology and role in regenerative medicine. *J. Dent. Res.* **88**, 792–806 (2009).
49. Kémoun, P. *et al.* Human dental follicle cells acquire cementoblast features under stimulation by BMP-2/-7 and enamel matrix derivatives (EMD) in vitro. *Cell Tissue Res.* **329**, 283–294 (2007).
50. Mehmet, E. *et al.* Comparison and optimisation of transfection of human dental follicle cells, a novel source of stem cells, with different chemical methods and electro-poration. *Neurochem Res.* **34**, 1272–1277 (2009).
51. Irie, T. *et al.* Intracellular transport of basement membrane-type heparan sulphate proteoglycan in adenoid cystic carcinoma cells of salivary gland origin: an immunoelectron microscopic study. *Virchows Arch.* **433**, 41–48 (1998).

Acknowledgments

We are grateful to Y. Shin and T. Takasu (Yamahachi Dental Mfg., Co., Aichi, Japan) for the hydroxyapatite coating of the dental implant. We also thank Y. Ochiai, N. Yamamoto and R. Koitabashi for their technical assistance. This work was supported by Organ Technologies Inc. We also received partial support from the Health and Labour Sciences Research Grants program from the Ministry of Health, Labour, and Welfare (No.21040101) to A.Y. (Tokyo Medical and Dental University) and a Grant-in-Aid for Scientific Research (A) from MEXT, Medicine, Dentistry and Pharmacy (No. 20249078) to T. Tsuji (2008–2010) from the Ministry of Education, Culture, Sports and Technology, Japan.

Author contributions

T. Tsuji and M. Oshima designed the research plan. M. Oshima, K.N., K.I., A.S., M.O. and T. Isobe performed the experiments. M. Oshima, T.T., S.K., T.T.-Y., T.I., M.S., K.T., T.K., A.Y. and T. Tsuji developed the new assay systems and wrote the discussion of the results. K.N., H.Y., C.T. and T.T. analysed the data. M. Oshima and T. Tsuji wrote the paper.

Additional information

Supplementary information accompanies this paper at http://www.nature.com/scientificreports

Competing financial interests: The authors declare no competing financial interests.

How to cite this article: Oshima, M. *et al.* Functional tooth restoration by next-generation bio-hybrid implant as a bio-hybrid artificial organ replacement therapy. *Sci. Rep.* **4**, 6044; DOI:10.1038/srep06044 (2014).

Biochemical and Biophysical Research Communications xxx (2014) xxx–xxx

Contents lists available at ScienceDirect

Biochemical and Biophysical Research Communications

journal homepage: www.elsevier.com/locate/ybbrc

Therapeutic potential of human adipose tissue-derived multi-lineage progenitor cells in liver fibrosis

Hanayuki Okura [a,b], Mayumi Soeda [a], Mitsuko Morita [a], Maiko Fujita [a], Kyoko Naba [a], Chiyoko Ito [a], Akihiro Ichinose [c], Akifumi Matsuyama [a,b,*]

[a] Platform of Therapeutics for Rare Disease, National Institute of Biomedical Innovation, 5-5-2-602 Minatojima-minamimachi, Chuo-ku, Kobe, Hyogo 650-0047, Japan
[b] The Center for Medical Engineering and Informatics, Osaka University, 2-2 Yamada-oka, Suita, Osaka 565-0879, Japan
[c] Department of Plastic Surgery, Kobe University Hospital, 7-5-2 Kusunoki-cho, Chuo-ku, Kobe, Hyogo, Japan

ARTICLE INFO

Article history:
Received 22 November 2014
Available online xxxx

Keywords:
hADMPCs
Chronic hepatitis
Fibrosis
MMPs
Mouse

ABSTRACT

Introduction: Liver fibrosis is characterized by excessive accumulation of extracellular matrix. In a mouse model of liver fibrosis, systemic injection of bone marrow mesenchymal stem cells (BM-MSCs) was considered to rescue the diseased phenotype. The aim of this study was to assess the effectiveness of human adipose tissue-derived multi-lineage progenitor cells (hADMPCs) in improving liver fibrosis.
Methods and results: hADMPCs were isolated from subcutaneous adipose tissues of healthy volunteers and expanded. Six week-old male nude mice were treated with carbon tetra-chloride (CCl_4) by intraperitoneal injection twice a week for 6 weeks, followed by a tail vein injection of hADMPCs or placebo control. After 6 more weeks of CCl_4 injection (12 weeks in all), nude mice with hADMPCs transplants exhibited a significant reduction in liver fibrosis, as evidenced by Sirius Red staining, compared with nude mice treated with CCl_4 for 12 weeks without hADMPCs transplants. Moreover, serum glutamic pyruvate transaminase and total bilirubin levels in hADMPCs-treated nude mice were lower levels than those in placebo controls. Production of fibrinolytic enzyme MMPs from hADMPCs were examined by ELISA and compared to that from BM-MSCs. MMP-2 levels in the culture media were not significantly different, whereas those of MMP-3 and -9 of hADMPCs were higher than those by BM-MSCs.
Conclusion: These results showed the mode of action and proof of concept of systemic injection of hADMPCs, which is a promising therapeutic intervention for the treatment of patients with liver fibrosis.

1. Introduction

Various conditions such as viral hepatitis, chronic alcohol abuse, metabolic diseases, autoimmune diseases and bile duct epithelial injury can cause liver fibrosis [1,2]. Liver fibrosis is reversible, whereas cirrhosis, the end-stage result of fibrosis, is in general irreversible [3]. Liver fibrosis is characterized by excessive accumulation of extracellular matrix, with the formation of scar tissue encapsulating the area of injury [4]. The prognosis of patients with liver fibrosis is poor, but liver transplantation seems to improve the prognosis [5,6]. However, limited numbers of donor livers are available for the millions of patients who need them worldwide [7]. Thus, there is a need for novel therapeutic approaches.

Recently, cell therapy has been proposed as an attractive tool for treatment of patients with severe liver disease [8–13]. Stem/progenitor cells, which possess certain characteristics including self-renewal, proliferation, longevity, and differentiation, are valuable in cell therapy [14]. Several groups have demonstrated the effectiveness of bone marrow-derived mesenchymal stem cells (BM-MSCs) in animal models of liver fibrosis and cirrhosis [15–18]. However, others have reported the lack of any changes in the extent of liver fibrosis or liver function tests following the use of BM-MSCs in a rat model of severe chronic liver injury [19]. Thus, the therapeutic efficacy of BM-MSCs transplantation remains controversial at present [19].

Adipose tissue-derived progenitor/stem cells are an attractive cell source for cell therapy of liver fibrosis, based on several properties of these cells; (1) ample production of fibrinolytic enzymes and cytokines [20], (2) ease of obtaining stem cells compared to other tissue-specific stem cells including BM-MSCs, [21]. The use of human adipose tissue-derived multi-lineage progenitor cells (hADMPCs) supports the view that cytokine production could mediate the therapeutic actions of hADMPCs in liver fibrosis.

* Corresponding author at: Platform of Therapeutics for Rare Diseases, National Institute of Biomedical Innovation, 5-5-2-602 Minatojima-minamimachi, Chuo-ku, Kobe, Hyogo 650-0047, Japan. Fax: +81 78 304 6176.
E-mail address: akifumi-matsuyama@umin.ac.jp (A. Matsuyama).

http://dx.doi.org/10.1016/j.bbrc.2014.11.122
0006-291X/

Please cite this article in press as: H. Okura et al., Therapeutic potential of human adipose tissue-derived multi-lineage progenitor cells in liver fibrosis, Biochem. Biophys. Res. Commun. (2014), http://dx.doi.org/10.1016/j.bbrc.2014.11.122

In the present study, we investigated the efficacy of treatment using hADMPCs in nude mice with CCl_4-induced chronic liver dysfunction and the mechanism of their action in improvement of liver fibrosis.

2. Materials and methods

2.1. Adipose tissue

Adipose tissue samples were resected from 7 human subjects during plastic surgery (all females, age, 20–60 years) as excess discards. About 10–50 g subcutaneous adipose tissue was collected from the sample of each subject. All subjects provided informed consent. The protocol was approved by the Review Board for Human Research of Kobe University, Graduate School of Medicine, Osaka University, Graduate School of Medicine and National Institute of Biomedical Innovation, Japan.

2.2. Isolation and expansion of hADMPCs

hADMPCs were prepared as described previously [8–10]. Briefly, the resected excess adipose tissue was minced and then digested at 37 °C for 1 h in Hank's balanced salt solution (HBSS, GIBCO Invitrogen, Grand Island, NY) with Liberase (Roche Diagnostics, Germany) as indicated by the manufacturer. Digests were filtered through a cell strainer (BD Bioscience, San Jose, CA) and centrifuged at 800×g for 10 min. Red blood cells were excluded using density gradient centrifugation with Lymphoprep (d = 1.077; Nycomed, Oslo, Norway), and the remaining cells were cultured in Dulbecco's modified Eagle's medium (DMEM, GIBCO Invitrogen) with 10% defined fetal bovine serum (FBS, Biological Industries, Israel) for 24 h at 37 °C. Following incubation, the adherent cells were washed extensively and then treated with 0.2 g/l ethylenediaminetetraacetate (EDTA) solution (Nacalai Tesque, Kyoto, Japan). The resulting suspended cells were replated on retronectin (RN)-coated dishes (Takara, Kyoto, Japan) in SteMedis (Nipro, Osaka, Japan), 1× insulin-transferring selenium (Nipro, Osaka), 1 nM dexamethasone (MSD, Tokyo, Japan), 100 μM ascorbic acid 2-phosphate (Sawai Pharmaceuticals Co., Osaka), 10 ng/ml epidermal growth factor (EGF, PeproTec, Rocky Hill, NJ), and 5% FBS (FBS, Biological Industries, Israel). The culture medium was changed twice a week and then the cells were applied for the experiments after 5–6 passages.

2.3. Flow cytometric analysis of hADMPCs

hADMPCs were characterized by flow cytometry. Cells were detached and stained with anti-human CD31, CD34, CD44, CD45, CD56, CD73, CD90, CD105 or CD166 antibodies (BD Lyoplate™ Screening Panels, BD Bioscience, San Jose, CA). Isotype-identical antibodies served as controls. After washing with Dulbecco's phosphate-buffered saline (PBS, Nacalai Tesque), cells were incubated with PE-labeled goat anti-mouse Ig antibody (BD PharMingen) for 30 min at 4 °C. After three washes, the cells were resuspended in PBS and analyzed by flow cytometry using a guava easyCyte flow cytometry systems (Merck Millipore, Darmstadt, Germany).

2.4. Adipogenic, osteogenic and chondrogenic differentiation procedure

Tri-lineage differentiation was examined as described previously [22]. Briefly, for adipogenic differentiation, the cells were cultured in Differentiation Medium (Zen-Bio, Inc.). After three days, half of the medium was replaced with Adipocyte Medium (Zen-Bio, Inc.) every two days. Five days after differentiation, characterization of adipocytes was confirmed by microscopic observation of intracellular lipid droplets after Oil Red O staining. Osteogenic differentiation was induced by culturing the cells in DMEM containing 10 nM dexamethasone, 50 mg/dl ascorbic acid 2-phosphate, 10 mM β-glycerophosphate (Sigma), and 10% FBS. Differentiation was examined by Alizarin red staining. For chondrogenic differentiation, 2×10^5 cells of the hADMPCs were centrifuged at 400×g for 10 min. The resulting pellets were cultured in chondrogenic medium (α-MEM supplemented with 10 ng/ml TGF-β, 10 nM dexamethasone, 100 M ascorbate, and 10 μl/ml 100× ITS Solution) for 14 days. For Alcian Blue staining, nuclear counter-staining with Weigert's hematoxylin was followed by 0.5% Alcian Blue 8GX for proteoglycan-rich cartilage matrix.

2.5. Animal model of liver fibrosis and cell administration

Chronic liver fibrosis was induced in nude mice using the procedure described previously [23,24] with some modification. Briefly, 6-week-old male nude mice (body weight of 20–30 g purchased from CLEA, Tokyo) were treated with a mixture of CCl_4 (Wako Pure Chemicals, Osaka) (0.3 ml/kg) and olive oil (Wako Pure Chemicals) (1:1 vol/vol) by intra-peritoneal injection twice a week for 6 weeks, and this was followed by a tail vein injection of hADMPCs (1.0×10^6 cells/kg body weight, n = 4) or placebo control (n = 5), and followed by 6 more weeks of CCl_4 treatment.

2.6. Liver function tests and histological analysis

Blood specimens were collected by cardiac puncture at the end of the experiment. Measurement of serum albumin, alanine aminotransferase (ALT), aspartate aminotransferase (AST), and total-bilirubin levels by routine laboratory methods was outsourced to Oriental Yeast Co. (Shiga, Japan).

Hematoxylin and eosin (H&E) staining and Sirius Red (SR) staining were performed to determine the extent of liver inflammation and fibrosis. The stained slides were viewed on a BioZero laser scanning microscope (Keyence, Osaka). The area of liver fibrosis was quantified with SR staining. Briefly, the fibrotic area (red staining) was assessed at 40× magnification using computer-assisted image analysis with All-in-One analysis software (Keyence, Osaka). Sixteen fields were randomly selected for each group.

2.7. Measurement of MMP-2, -3 and -9 production by hADMPCs

One million cells of hADMPCs and BM-MSCs (DS Pharma Biomedical, Osaka) were seeded onto 6 well plates and then cultured for 24 h. The supernatants were harvested, centrifuged, and frozen at −80 °C until analysis. MMP-2, MMP-3 and MMP-9 were measured by enzyme-linked immunosorbent assay (ELISA) kits from R&D Systems (Minneapolis, MN) using the instructions supplied by the manufacturer.

2.8. Statistical analysis

Serum parameters and fibrotic area are presented as mean ± SD. Differences between groups were assessed for statistical significance by the Student's t-test, with $p < 0.05$ considered statistically significant.

3. Results

3.1. Characterization of hADMPCs

Flow cytometry was used to assess markers expressed by hADMPCs (Fig. 1A). The cells were negative for markers of

Please cite this article in press as: H. Okura et al., Therapeutic potential of human adipose tissue-derived multi-lineage progenitor cells in liver fibrosis, Biochem. Biophys. Res. Commun. (2014), http://dx.doi.org/10.1016/j.bbrc.2014.11.122

hematopoietic lineage (CD45) and hematopoietic stem cells, CD34 and CD133. They were also negative for CD31, an endothelial cell-associated marker, and c-Kit (CD117), a cell surface antigen. However, they stained positively for several surface markers characteristic of mesenchymal stem cells, but not embryonic stem (ES) cells, such as CD29, CD44 (hyaluronan receptor), CD73 and CD105 (endoglin).

Next, we examined the adipogenic, osteogenic and chondrogenic differentiation potentials of hADMPCs. Adipogenic differentiation was confirmed by accumulation of intracellular lipid droplets stained with Oil Red O (Fig. 1B). Differentiation and induction of hADMPCs was associated with increase in the amount of Oil Red O-stained lipid droplets, indicating that hADMPCs can differentiate into adipocytes. Osteogenic induction was examined by Alizarin red S staining (Fig. 1B). Induction of hADMPCs for osteogenesis was associated with Alizarin red S staining and appearance of mineralized nodules. The chondrogenic potential of hADMPCs is shown in Fig. 1B. Induction of chondrogenesis by pellet culture resulted in staining of extracellular matrices of hADMPCs-derived pellet-cultured chondrocytes for Alcian Blue, indicating the chondrogenic differentiation potential of hADMPCs. These results confirmed the tri-lineage differentiation potential of hADMPCs and the mesenchymal stem cell properties of hADMPCs.

3.2. Effects of hADMPC on CCl_4-induced chronic liver dysfunction in nude mice

We adopted the CCl_4-induced chronic mouse fibrosis model in this study rather than the CCl_4-induced acute model because CCl_4-induced acute liver fibrosis resolves spontaneously [25]. For this purpose, 9 male nude mice were injected intraperitoneally with CCl_4 twice weekly for 6 weeks, and then divided into two groups, 4 animals received hADMPCs transplantation via the tail vein and the other 5 vehicle control received Ringer's solution with 1/30 volume of heparin. All animals were followed for 6 weeks after the last injection (a).

H&E staining of liver sections showed reduced hepatocyte vacuolar degeneration in hADMPC-transplanted CCl_4-injured mice compared with the control (Fig. 2B). The peri-lobular regions were the main areas affected by CCl_4 hepatotoxicity while the centrilobular regions seemed to be the least affected. These findings suggest intact albumin secretion, which was confirmed by Sirius Red (SR) staining of control liver sections. SR staining of sections from hADMPC-transplanted mice showed mild liver fibrosis, while that of sections from control group mice showed moderate fibrosis (Fig. 2B). Quantitative image analysis of the fibrotic area in SR-stained sections confirmed the efficacy of hADMPC-transplantation on liver fibrosis. The mean fibrotic area was significant lower in hADMPC-transplanted CCl_4-injured mice ($1.8 \pm 1.1\%$ of fibrotic areas) than control mice ($10.9 \pm 3.9\%$ of fibrotic areas) ($p < 0.05$), indicating that hADMPC-transplantation ameliorated liver fibrosis and increased the area containing hepatocytes (c).

3.3. Functional recovery of liver damage following transplantation of hADMPCs

We next evaluated the effects of cell transplantation on the extent of liver injury and liver function. Serum transaminase levels (AST and ALT) were significantly higher in mice with liver damage (control), but the increase was attenuated by hADMPCs transplantation (Fig. 3A and B). These results confirmed the effectiveness of hADMPCs in the treatment of liver damage associated with fibrosis.

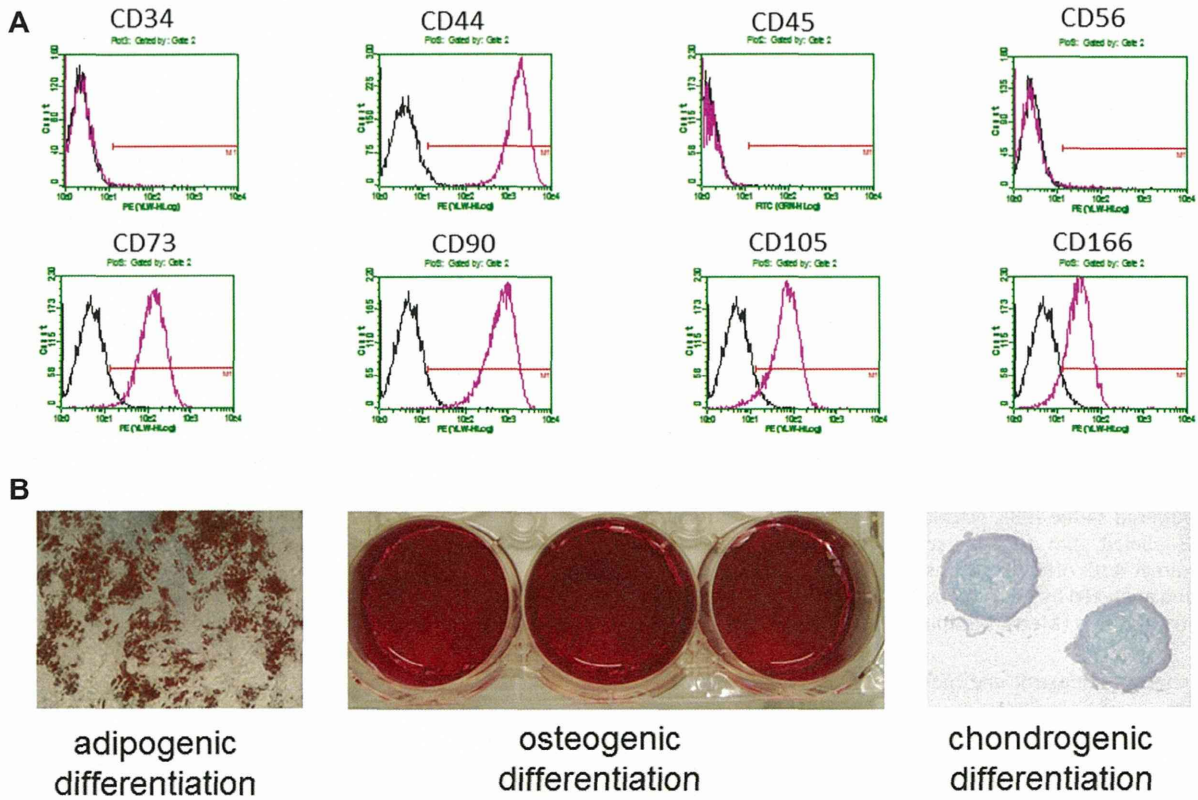

Fig. 1. Characterization of hADMPCs. (A) Flow cytometric characterization of hADMPCs. (B) An isotype-matched negative control indicated as red curve. (C) Adipogenic, osteogenic and chondrogenic differentiation potentials of hADMPCs. (For interpretation of the references to color in this figure legend, the reader is referred to the web version of this article.)

Please cite this article in press as: H. Okura et al., Therapeutic potential of human adipose tissue-derived multi-lineage progenitor cells in liver fibrosis, Biochem. Biophys. Res. Commun. (2014), http://dx.doi.org/10.1016/j.bbrc.2014.11.122

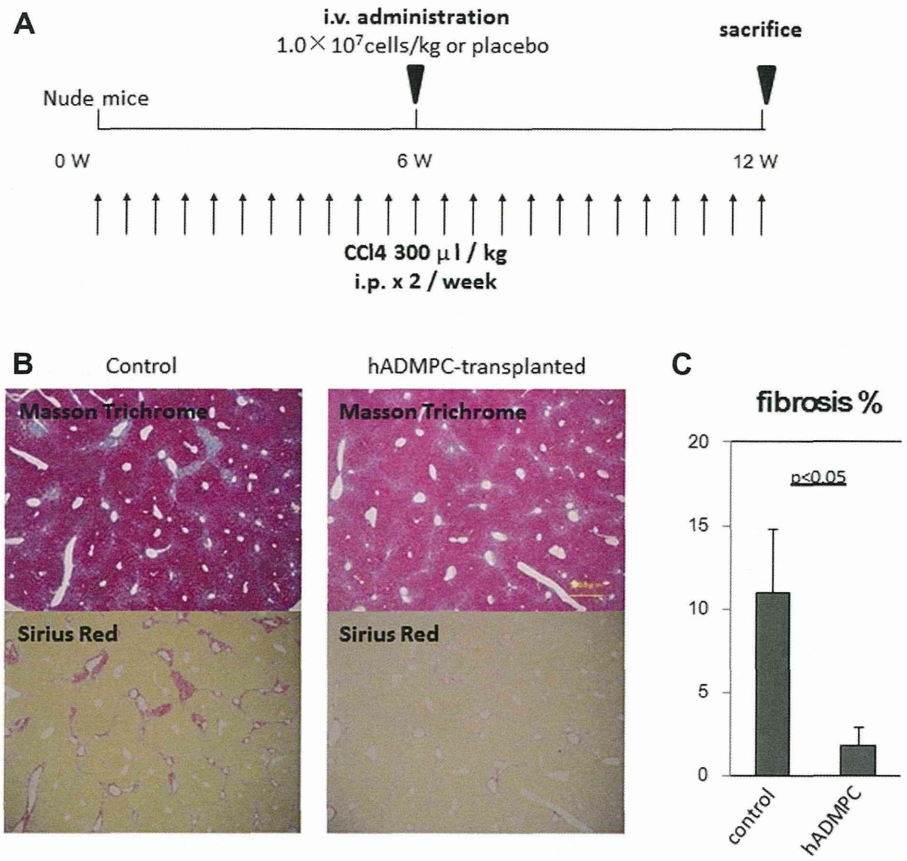

Fig. 2. Assessment of liver fibrosis in hADMPC-transplanted nude mice and controls. (A) Diagram of the treatment protocol. (B) Extracellular deposition of collagen fibers stained with Sirius Red. (C) Quantification of collagen by image analysis. (For interpretation of the references to color in this figure legend, the reader is referred to the web version of this article.)

Interestingly, serum albumin level remained high after hADMPCs, similar to the control (Fig. 3C). These results could be explained by damage of the centrilobular region, the main site of albumin production. Considered together, the results suggest the beneficial effects of hADMPCs in attenuating liver damage and recovery of liver function.

3.4. hADMPCs-induced functional recovery is mediated by MMP release

Finally, we analyzed the mechanism of the hepatoprotective effect of hADMPCs. For this purpose, we measured the amount of the fibrinolytic enzymes, MMP-2, MMP-3 and MMP-9, secreted by hADMPCs by ELISA (Fig. 4). After 3-day culture, the amounts of enzymes production by hADMPCs and BM-MSCs were measured. There was no significant difference in MMP-2 production by hADMPCs and BM-MSCs (59.7 ± 2.3 vs 58.3 ± 0.0 ng/ml from 1.0×10^4 cells cultured for 3 days). On the other hand, MMP-3 and MMP-9 production levels were significantly higher in hADMPCs than BM-MSCs (6.84 ± 2.3 vs 0.03 ± 0.0 ng/ml, $p < 0.05$, 0.462 ± 0.015 vs 0.003 ± 0.008 ng/ml, $p < 0.05$, from 1.0×10^4 cells cultured for 3 days, respectively).

4. Discussion

The major finding of the present study was improvement of liver fibrosis in CCl_4-induced mice after systemic administration of hADMPCs, and that this effect was mediated, at least in part, through the production of fibrinolytic MMP-2, -3, and -9, from hADMPCs, suggesting that these cells could be particularly effective in resolving liver fibrosis.

Liver transplantation is an established treatment for severe liver cirrhosis, although the number of patients who could benefit from such treatment is small due to the limited number of donors [5]. Cell therapy has been proposed as an alternative and attractive tool for treating patients with severe liver disease [8–13]. Among the cell therapy tested so far, hepatocyte replacement therapy had been examined. Isolated hepatocytes from human liver [13], regenerated hepatocyte-like or –progenitor cells from embryonic, induce pluripotent [26,27], or hepatic progenitor cells [11], and *in situ* reprogrammable cells (9, 10) have been tested for their efficacy in animal models. The strategy has also been successful in clinical trials involving patients with certain inherited diseases [28]. Although large numbers of hepatocytes or hepatocyte-like cells are needed for meaningful cure and there should be no room for the cells in fibrotic hepatic parenchyma to engraft, such replacement therapies, however, do not seem to be clinically fruitful for liver fibrosis. We hypothesized that fibrolytic enzymes produced by hADMPCs could be useful for treatment of liver fibrosis, and therefore shifted the treatment strategy to improvement of liver fibrosis with cell-based fibrinolytic enzymes delivery. In this strategy, hADMPCs derived-MMPs should produce lysis of excess extracellular matrices and make room for the patient's own proliferative hepatocytes.

To establish the cell-based fibrinolytic enzyme delivery therapy as first line next to liver transplantation, some challenging issues

Please cite this article in press as: H. Okura et al., Therapeutic potential of human adipose tissue-derived multi-lineage progenitor cells in liver fibrosis, Biochem. Biophys. Res. Commun. (2014), http://dx.doi.org/10.1016/j.bbrc.2014.11.122

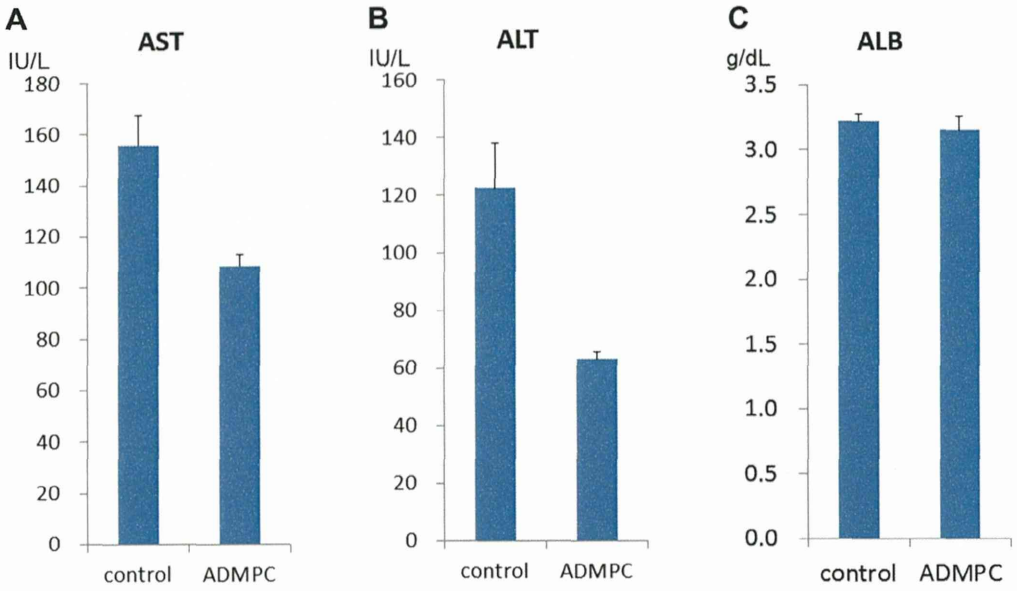

Fig. 3. Examination of serum parameters. (A, B) Transaminase (AST and ALT), (C) Serum albumin. Data are mean ± SD. C: control mice; T: mice transplanted mice with hADMPCs.

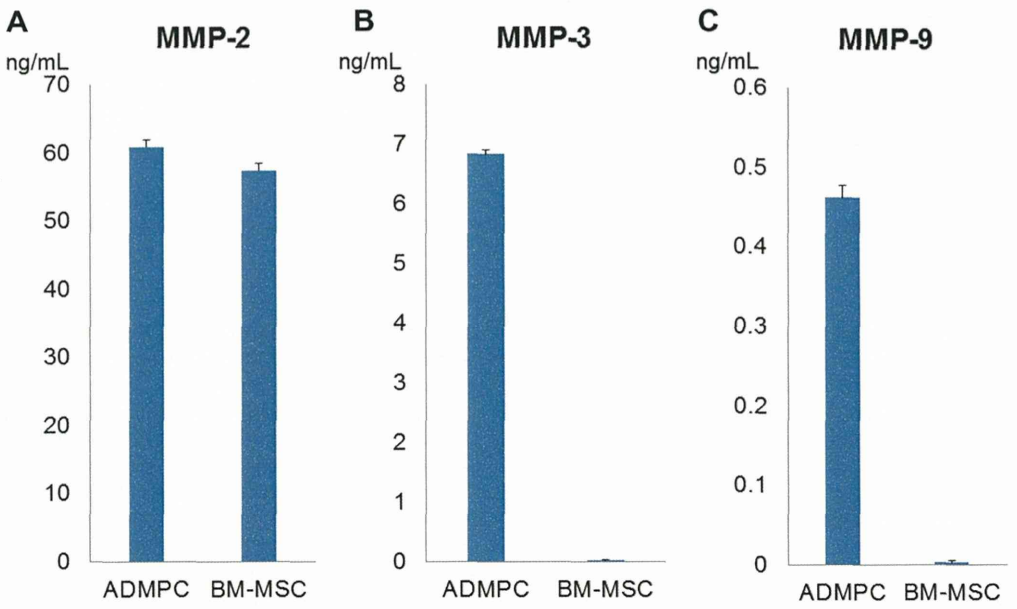

Fig. 4. Quantitative analysis of MMP-2, MMP-3 and MMP-9 level produced by hADMPCs and BM-MSCs. The amount of MMP-2 (A), MMP-3 (B) and MMP-9 (C) after 3 days of culture.

should be dealt with; (1) the cells should be obtained easily and ethically in large quantities, (2) the cells should improve liver fibrosis and liver panel, and (3) the cells act as vehicle for the delivery of MMPs.

The first issue is whether the cells could be obtained easily and ethically in large quantities. hADMPCs is favorable for the therapy because adipose tissue, from which ADMPCs are obtained, is easily and safely accessible and large quantities of the tissues can be obtained without serious ethical issues, since liposuction surgery yields from 100 ml to >3 L of lipoaspirate tissue [8–10]. Therefore, hADMPCs can potentially be applied not only for autologous but also allogenic cell-based enzyme delivery in the future. Based on the above advantages, hADMPCs represent a potentially promising source of cells for the therapy.

Second, we need to show that hADMPCs-administration results in improvement of liver fibrosis and liver panel, as proof-of-concept of therapy. As shown in Fig. 2, hADMPC significantly improved liver fibrosis in CCl_4-treated nude mice (a model of chronic liver cirrhosis). The treatment also resulted in improvement of serum transaminase levels. In this model, massive fibrosis was mainly noted in the peri-hepatic lobular region but not in the centrilobular regions surrounding the central veins. Albumin is known to be mainly produced by hepatocytes in the centrilobular region. This is the most likely reason for the lack of difference in serum albumin

Please cite this article in press as: H. Okura et al., Therapeutic potential of human adipose tissue-derived multi-lineage progenitor cells in liver fibrosis, Biochem. Biophys. Res. Commun. (2014), http://dx.doi.org/10.1016/j.bbrc.2014.11.122

levels between hADMPC-transplanted animals and controls. These results indicate that hADMPCs transplantation showed the proof-of-concept to liver dysfunction associated with fibrosis.

Finally, an important issue in this kind of therapy is whether the cells secrete sufficient amount of MMPs. One study reported that matrix metalloproteinase gene delivery could decrease collagen fibers and reduce liver fibrosis [29]. The mode of action was considered to be the strong expression MMPs on the transplanted cells, indicating that MMPs-producing cells other than BM-MSCs [30] are suitable for use for the cell-based enzyme delivery. The present study showed that hADMPCs expressed MMP-2, -3 and -9 (Fig. 2). There was no significant difference in MMP-2 production between hADMPC and BM-MSCs. However, the production of MMP-3 and MMP-9 from hADMPCs was superior to that from BM-MSCs. MMP-3 and MMP-9 are known to lyse collagen types III and I, which are major compartment of liver fibrotic lesion [29]. These data highlight the potential effectiveness of hADMPCs in the treatment of liver fibrosis and the superiority of hADMPCs compared to other therapies.

In conclusion, the present study demonstrated that systemic administration of hADMPCs significantly attenuated liver fibrosis and improved liver function, and that the therapeutic effect of hADMPCs was in part due the secretion of fibrinolytic enzymes, MMPs. These proofs of concept and mode of action prompted us to choose hADMPCs for cell therapy of liver fibrosis. hADMPCs therapy, as cell-based enzyme delivery therapy, has the potential to be an effective source of inducers that support liver regeneration.

Declaration

The authors declare no conflict of interest.

Acknowledgments

This study was partly supported by a grant-in-aid for A.M. from the Ministry of Health, Labor and Welfare, Japan.

References

[1] A. Kasahara, H. Tanaka, T. Okanoue, et al., Interferon treatment improves survival in chronic hepatitis C patients showing biochemical as well as virological responses by preventing liver-related death, J. Viral Hepat. 11 (2004) 148–156.
[2] T. Saito, K. Misawa, S. Kawata, Intern. Med. 6 (2007) 101–103.
[3] V. Manne, E. Akhtar, S. Saab, J. Clin. Gastroenterol. 8 (2014) e76–e84.
[4] A. Mallat, S. Lotersztajn, Am. J. Physiol. Cell Physiol. 305 (2013) C789–C799.
[5] C.L. Chen, S.T. Fan, S.G. Lee, et al., Living-donor liver transplantation: 12 years of experience in Asia, Transplantation 75 (2003) S6–S11.
[6] Y. Takada, M. Ueda, T. Ito, Living donor liver transplantation as a second-line therapeutic strategy for patients with hepatocellular carcinoma, Liver Transpl. 12 (2006) 912–919.
[7] R. Rai, Liver transplantation – an overview, Indian J. Surg. 75 (2013) 185–191.
[8] H. Okura, H. Komoda, A. Saga, Tissue Eng. Part C Methods 16 (2010) 761–770.
[9] H. Okura, A. Saga, Y. Fumimoto, Tissue Eng. Part C Methods 17 (2011) 145–154.
[10] A. Saga, H. Okura, M. Soeda, HMG-CoA reductase inhibitor augments the serum total cholesterol-lowering effect of human adipose tissue-derived multilineage progenitor cells in hyperlipidemic homozygous Watanabe rabbits, Biochem. Biophys. Res. Commun. 412 (2011) 50–54.
[11] R. Semeraro, V. Cardinale, G. Carpino, et al., The fetal livers as cell source for the regenerative medicine of liver and pancreas, Ann. Transl. Med. 1 (2013) 13.
[12] K. Sun, X. Xie, J. Xi, et al., Cell-based therapy for acute and chronic liver failures: distinct diseases, different choices, Sci. Rep. 4 (2014) 6494.
[13] C. Jorns, E.C. Ellis, G. Nowak, et al., Hepatocyte transplantation for inherited metabolic diseases of the liver, J. Intern. Med. 272 (2012) 201–223.
[14] M.F. Pittenger, A.M. Mackay, S.C. Beck, et al., Multilineage potential of adult human mesenchymal stem cells, Science 284 (1999) 143–147.
[15] T. Saito, K. Okumoto, H. Haga, et al., Potential therapeutic application of intravenous autologous bone marrow infusion in patients with alcoholic liver cirrhosis, Stem Cells Dev. 20 (2011) 1503–1510.
[16] I. Sakaida, Autologous bone marrow cell infusion therapy for liver cirrhosis, J. Gastroenterol. Hepatol. 3 (2008) 1349–1353.
[17] M. Abdel Aziz, H. Atta, S. Mahfouz, Therapeutic potential of bone marrow-derived mesenchymal stem cells on experimental liver fibrosis, 2007, Clin. Biochem. 40 (2007) (2007) 893–899.
[18] M. Hardjo, M. Miyazaki, M. Sakaguchi, et al., Suppression of carbon tetrachloride-induced liver fibrosis by transplantation of a clonal mesenchymal stem cell line derived from rat bone marrow, Cell Transplant. 18 (2009) 89–99.
[19] A.B. Carvalho, L.F. Quintanilha, J.V. Dias, et al., Bone marrow multipotent mesenchymal stromal cells do not reduce fibrosis or improve function in a rat model of severe chronic liver injury, Stem Cells 26 (2008) 1307–1314.
[20] Y. Ding, D. Xu, G. Feng, et al., Mesenchymal stem cells prevent the rejection of fully allogenic islet grafts by the immunosuppressive activity of matrix metalloproteinase-2 and -9, Diabetes 58 (2009) 1797–1806.
[21] J.M. Gimble, B.A. Bunnell, T. Frazier T, et al., Adipose-derived stromal/stem cells: a primer, Organogenesis 9 (2013) 3–10.
[22] H. Komoda, H. Okura, C.-M. Lee, et al., Reduction of N-glycolylneuraminic acid xenoantigen on human adipose tissue-derived stromal cells/mesenchymal stem cells leads to safer and more useful cell sources for various stem cell therapies, Tissue Eng. Part A 16 (2010) 1143–1155.
[23] I. Sakaida, S. Terai, N. Yamamoto, et al., Transplantation of bone marrow cells reduces CCl_4-induced liver fibrosis in mice, Hepatology 40 (2004) 1304–1311.
[24] T. Takami, S. Terai, I. Sakaida, Advanced therapies using autologous bone marrow cells for chronic liver disease, Discov. Med. 14 (2012) 7–12.
[25] L.W. Weber, M. Boll, A. Stampfl, Hepatotoxicity and mechanism of action of haloalkanes: carbon tetrachloride as a toxicological model, Crit Rev Toxicol. 33 (2003) 105–136.
[26] D.A. Chistiakov, P.A. Chistiakov, Strategies to produce hepatocytes and hepatocyte-like cells from pluripotent stem cells, Hepatol. Res. 42 (2012) 111–119.
[27] M. Imamura, T. Aoi, A. Tokumasu, et al., Induction of primordial germ cells from mouse induced pluripotent stem cells derived from adult hepatocytes, Mol. Reprod. Dev. 77 (2010) 802–811.
[28] J. Meyburg, G.F. Hoffmann, Liver, liver cell and stem cell transplantation for the treatment of urea cycle defects, Mol. Genet. Metab. 100 (Suppl. 1) (2010) S77–S83.
[29] Y. Iimuro, D.A. Brenner, Matrix metalloproteinase gene delivery for liver fibrosis, Pharm. Res. 25 (2008) 249–258.
[30] B. Usunier, M. Benderitter, R. Tamarat, A. Chapel, Management of fibrosis: the mesenchymal stromal cells breakthrough, Stem Cells Int. 2014 (2014) 340257.

Please cite this article in press as: H. Okura et al., Therapeutic potential of human adipose tissue-derived multi-lineage progenitor cells in liver fibrosis, Biochem. Biophys. Res. Commun. (2014), http://dx.doi.org/10.1016/j.bbrc.2014.11.122